



PERGAMON

Available online at www.sciencedirect.com

SCIENCE @ DIRECT®

Polyhedron 22 (2003) 1765–1769



POLYHEDRON

www.elsevier.com/locate/poly

# A new family of $Mn_{12}$ single-molecule magnets: replacement of carboxylate ligands with diphenylphosphinates

Jonathan T. Brockman<sup>a</sup>, Khalil A. Abboud<sup>a</sup>, David N. Hendrickson<sup>b</sup>,  
George Christou<sup>a,\*</sup>

<sup>a</sup> Department of Chemistry, University of Florida, Gainesville, FL 32611-7200, USA

<sup>b</sup> Department of Chemistry and Biochemistry, University of California at San Diego, La Jolla, Gilman Drive, CA 92083-0358, USA

Received 6 October 2002; accepted 28 October 2002

## Abstract

The synthesis, structural characterization and magnetic properties of a new mixed ligand member of the  $Mn_{12}$  family are reported. The reaction of  $[Mn_{12}O_{12}(O_2CPh)_{16}(H_2O)_4]$  (**4**) with diphenylphosphinic acid produces  $[Mn_{12}O_{12}(O_2CPh)_7(O_2PPh_2)_9(H_2O)_4]$  (**5**). The crystal structure of **5** shows the  $[Mn_{12}O_{12}]^{16+}$  core is retained and exhibits two abnormally oriented Jahn-Teller elongation axes. The ligand distribution alternates about the core with the ninth  $Ph_2PO_2^-$  group in an equatorial position. Magnetic studies indicate an  $S = 10$  ground state and retention of the single-molecule magnetism behavior.

© 2003 Elsevier Science Ltd. All rights reserved.

**Keywords:** Single-molecule magnets; Crystal structures; Magnetic properties

## 1. Introduction

Considerable interest exists at present in the field of single-molecule magnetism (SMM), the capability of an individual molecule to function as a nanoscale magnet. The first and most well studied example of a SMM was  $[Mn_{12}O_{12}(O_2CMe)_{16}(H_2O)_4] \cdot 4H_2O \cdot 2MeCO_2H$  (**1**) [1–3]. Owing to its large spin ground state ( $S = 10$ ) and a negative easy-axis magnetoanisotropy (negative zero-field splitting parameter  $D$ ), each molecule possesses an energy barrier ( $DS_2^2$ ) to the reversal of magnetization. At temperatures below the blocking temperature ( $T_B$ ), a SMM displays a hysteresis loop in magnetization versus DC field studies and frequency-dependent peaks in the out-of-phase component of an AC susceptibility measurement. SMMs have also advanced our understanding of the physics of nanoscale magnetic particles. The quantum effects predicted for magnetic particles at their miniaturization limit were finally observed. For example, resonant quantum tunneling of magnetization was

seen as steps in the magnetization hysteresis loop of **1** [4–6].

To further the understanding of these quantum effects, structural modifications to such molecules have been pursued to probe the influence on the magnetic properties. In the  $Mn_{12}$  area, synthetic procedures have been developed to replace the  $MeCO_2^-$  ligands of complex **1** with almost any other type of carboxylate group, leading to increased solubility in organic solvents and greatly altered redox properties [7,8]. Methods have also been developed to synthesize  $Mn_{12}$  molecules containing more than one type of peripheral bridging ligand. One strategy involved the site-specific replacement of carboxylates to form  $[Mn_{12}O_{12}(O_2CR)_8(O_2CR')_8(H_2O)_3]$  products [9]. Another synthetic approach selectively resulted in the replacement of four  $RCO_2^-$  groups with  $NO_3^-$  groups to give  $[Mn_{12}O_{12}(O_2CR)_{12}(NO_3)_4(H_2O)_4]$ , the first  $Mn_{12}$  to contain non-carboxylate bridging ligands [10]. Furthermore, eight diphenylphosphinate groups have been introduced to give  $[Mn_{12}O_{12}(O_2CMe)_8(O_2PPh_2)_8(H_2O)_4]$  (**2**) with both axial and equatorial  $Ph_2PO_2^-$  groups [11]. More recently, site-specific substitution of eight carboxylates with  $RSO_3^-$  ( $R = Ph$ ) groups has been accomplished [12].

\* Corresponding author. Tel.: +1-352-392-8314; fax: +1-352-392-8757.

E-mail address: christou@chem.ufl.edu (G. Christou).

Complex **2** exhibits the phenomenon of Jahn-Teller (JT) isomerism, defined as non-equivalent molecules differing in the relative orientation of one or more JT distortion axes [13,14]. This phenomenon significantly affects relaxation rates and gives significantly different positions of the out-of-phase AC susceptibility ( $\chi_M''$ ) signal. Complexes with abnormally oriented JT axes display faster relaxation rates [14].

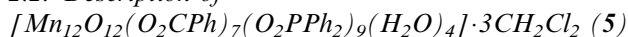
In the present work, we report the reaction of  $[\text{Mn}_{12}\text{O}_{12}(\text{O}_2\text{CPh})_{16}(\text{H}_2\text{O})_4]$  (**4**) with  $\text{Ph}_2\text{PO}_2\text{H}$ . The product  $[\text{Mn}_{12}\text{O}_{12}(\text{O}_2\text{CPh})_7(\text{O}_2\text{PPh}_2)_9(\text{H}_2\text{O})_4]$  (**5**) possesses two abnormally oriented JT axes. We describe the magnetic properties of this complex, and show that it is also a SMM.

## 2. Results and discussion

### 2.1. Synthesis

Reaction of eight equivalents of diphenylphosphinic acid with the benzoate substituted  $\text{Mn}_{12}$ , complex **4**, in  $\text{MeCN}/\text{CH}_2\text{Cl}_2$  (1:1) solution yields the new complex  $[\text{Mn}_{12}\text{O}_{12}(\text{O}_2\text{CPh})_7(\text{O}_2\text{PPh}_2)_9(\text{H}_2\text{O})_4]$  (**5**). Pure product was isolated in 45–50% yield after recrystallization from a layered mixture of  $\text{CH}_2\text{Cl}_2$ /hexanes. Full details will be provided elsewhere.

### 2.2. Description of



Complex **5** has a structure similar to complexes **1**, **2** and **4**, with a central  $[\text{Mn}_4^{\text{IV}}\text{O}_4]$  cubane held within a non-planar ring of eight  $\text{Mn}^{\text{III}}$  ions by eight  $\mu_3\text{-O}^{2-}$  ions. As for complex **2**, the axial  $\text{Mn}^{\text{III}}\text{-Mn}^{\text{III}}$  and four of the equatorial  $\text{Mn}^{\text{III}}\text{-Mn}^{\text{III}}$  carboxylate sites have been replaced with diphenylphosphinate groups. Additionally, however, complex **5** has a ninth diphenylphosphinate group bridging in an equatorial position. The remaining equatorial and the four axial  $\text{Mn}^{\text{III}}\text{-Mn}^{\text{IV}}$  sites are occupied by benzoates. Four water groups complete peripheral ligation, bound in the same 1:1:1:1 arrangement as found in **1** and **2**.

Crystals of complex **5** grown from  $\text{CH}_2\text{Cl}_2$ /hexanes were crystallographically characterized as  $5 \cdot 3 \text{CH}_2\text{Cl}_2$ , which crystallizes in the monoclinic space group  $C2/c$ . A labeled ORTEP plot is shown in Fig. 1. The  $\text{Mn}_{12}$  complex is located on a crystallographic twofold axis perpendicular to the  $\text{Mn}_{12}$  plane. One benzoate ligand is disordered with a diphenylphosphinate ligand where one phenyl group of the latter coincides with the phenyl group of the benzoate. Thus, the benzoate carbon atom ( $\text{C1}'$ ) is disordered with the  $\text{P}(\text{Ph})$  group ( $\text{P2}$ ). The site occupation factors of the disordered groups were refined independently to 0.56(1) for the  $\text{P}(\text{Ph})$  group, and consequently 0.44(1) for the benzoate carbon atom. There-

fore, the asymmetric unit consists of half a  $\text{Mn}_{12}$  cluster with 3.44 benzoate and 4.56 diphenylphosphinate groups as well as 1.5  $\text{CH}_2\text{Cl}_2$  solvate molecules.

The incorporation of the phosphinate groups causes a distortion of the  $[\text{Mn}_{12}\text{O}_{12}]^{16+}$  core in a manner very similar to complex **2** [11]; however, the ‘bowing’ effect of the linear  $\text{Mn}_4$  units is slightly less,  $174^\circ$  for **5** versus  $171\text{--}173^\circ$  for **2**.

Lastly, the  $\text{Mn}^{\text{III}}$  ions experience a JT elongation where two *trans* Mn-ligand distances are longer than those for the other four ligands. JT elongation axes avoid the shortest and strongest (usually  $\text{Mn}\text{-O}^{2-}$ ) bonds. The most common and expected orientation of the JT axes is approximately parallel to the axial direction of the molecule.  $[\text{Mn}_{12}\text{O}_{12}(\text{O}_2\text{CPh-}p\text{-Me})_{16}(\text{H}_2\text{O})_4]$  was the first  $\text{Mn}_{12}$  system found to possess a JT axis oriented perpendicular to the axial direction and towards an oxide ligand, thus described as an abnormal JT axes [13]. Complex **5** exhibits two abnormally oriented JT axes (on  $\text{Mn}4$  and  $\text{Mn}4'$ ). The magnetic properties of this molecule are thus expected to be similar with those of previously studied  $\text{Mn}_{12}$  systems with abnormally oriented JT axes.

### 2.3. DC magnetic susceptibility

Variable-temperature DC magnetic susceptibility ( $\chi_M$ ) data were collected for a microcrystalline sample of complex **5** in the 2.00–300 K range in a 10 kG magnetic field. The  $\chi_M T$  versus  $T$  behavior is similar to those of previously studied  $[\text{Mn}_{12}\text{O}_{12}(\text{O}_2\text{CR})_{16}(\text{H}_2\text{O})_4]$  complexes, and also the  $[\text{Mn}_{12}\text{O}_{12}(\text{O}_2\text{C-Me})_8(\text{O}_2\text{PPh}_2)_8(\text{H}_2\text{O})_4]$  complex [7,11]. The  $\chi_M T$  value increases with decreasing temperature from  $18.97 \text{ cm}^3 \text{ K mol}^{-1}$  at 300 K to a maximum of  $43.11 \text{ cm}^3 \text{ K mol}^{-1}$  at 20.0 K, whereupon there is a decrease to  $11.15 \text{ cm}^3 \text{ K mol}^{-1}$  at 2.00 K. The maximum indicates a large ground state spin ( $S$ ) value, and the rapid decrease at low temperature is primarily due to Zeeman and zero-field splitting effects.

To characterize the ground state of complex **5**, magnetization ( $M$ ) data were collected in the 1.80–10.0 K range with applied magnetic fields of 1.0–70 kG. A plot of the reduced magnetization ( $M/N\mu_B$ ) versus  $H/T$  is given in Fig. 2. The data were fit by diagonalization of the spin Hamiltonian matrix incorporating axial ZFS ( $DS_z^2$ ) and Zeeman interactions and assuming only the ground state to be populated at these temperatures [15]. The best fit is shown as solid lines in Fig. 3, and the fitting parameters were  $S = 10$ ,  $g = 1.83$ , and  $D = -0.42 \text{ cm}^{-1} = -0.60 \text{ K}$ . Complex **4** was also reported to have an  $S = 10$  ground state, with  $D = -0.50 \text{ cm}^{-1} = -0.72 \text{ K}$  [1]. Thus, the replacement of nine benzoate groups with nine  $\text{Ph}_2\text{PO}_2^-$  groups does not change the ground state, a result consistent with the

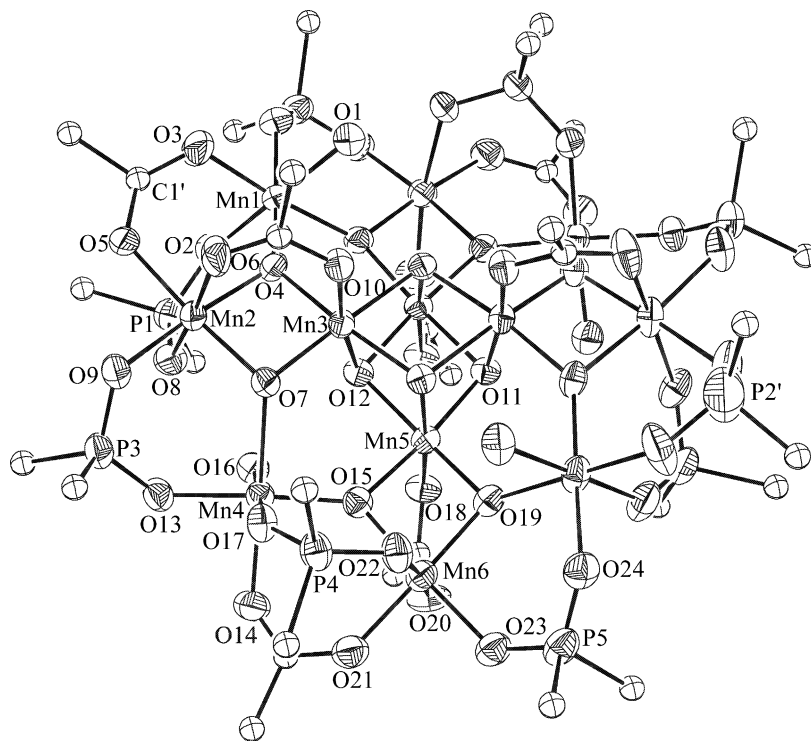


Fig. 1. ORTEP representation of complex **5** showing 50% probability ellipsoids. For clarity, only the *ipso* carbons of the phenyl rings are shown and all hydrogen atoms have been omitted.

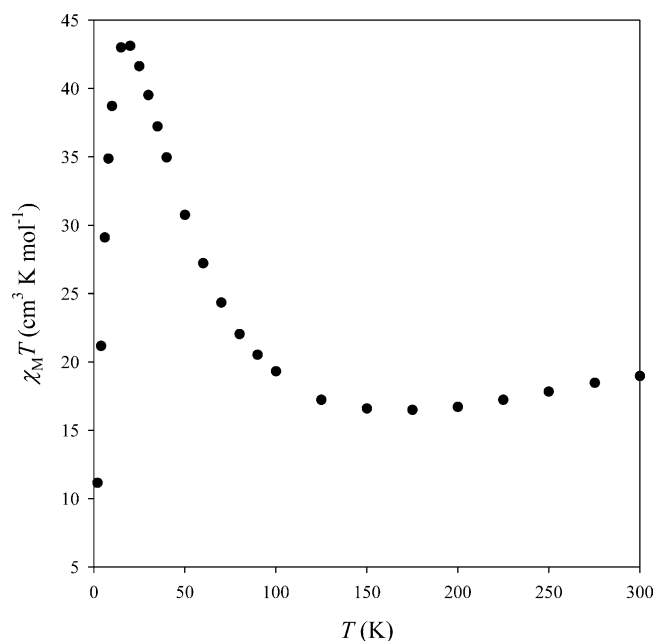


Fig. 2. Plot of the  $\chi_M T$  of complex **5** versus temperature.

minimal structural perturbation of the core resulting from the ligand replacement.

#### 2.4. AC magnetic susceptibility

AC magnetic susceptibility data were collected for complex **5** in the 1.8–10.0 K range in a 3.5 G AC field

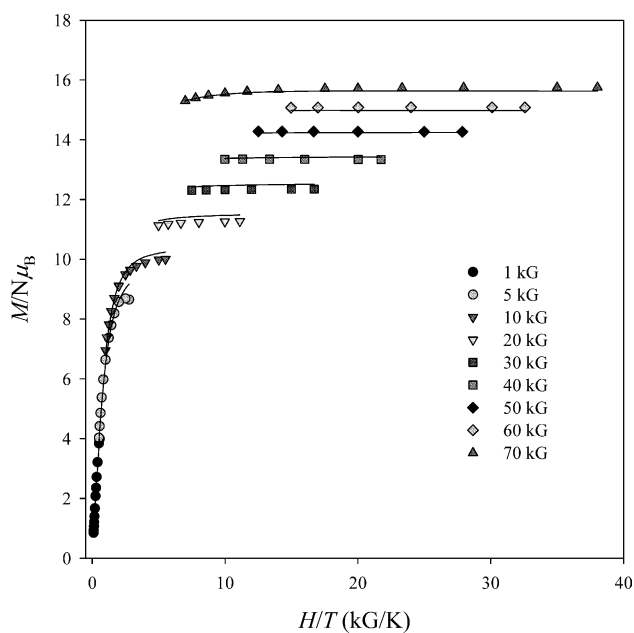


Fig. 3. Plot of  $M/N\mu_B$  versus  $H/T$  for complex **5** at different fields. The solid line represents the best fit as described in the text.

oscillating at 4–1500 Hz. Plots of the in-phase component ( $\chi'_M$ , plotted as  $\chi'_M T$ ) and the out-of-phase component ( $\chi''_M$ ) versus  $T$  at eight different frequencies are shown in Fig. 4. The  $\chi'_M T$  signal shows a frequency-dependent decrease at  $T < 5$  K, indicative of the onset of slow relaxation. The  $\chi'_M T$  value remains relatively

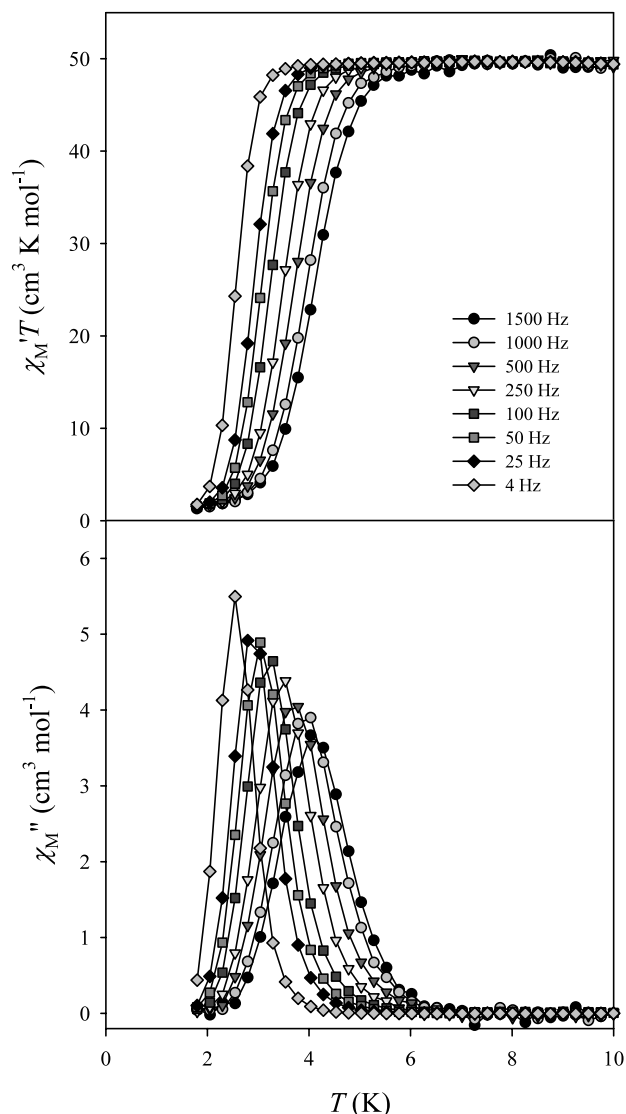


Fig. 4. Plot of the AC magnetic susceptibility data for complex **5** showing the in-phase ( $\chi'_M$ ) (top) and out-of-phase ( $\chi''_M$ ) (bottom) signals versus temperature.

constant at a value of  $49 \text{ cm}^3 \text{ K mol}^{-1}$  between 10 and 3–4 K. Below this, the value of  $\chi'_M T$  decreases rapidly. Simultaneously with the sharp decrease in  $\chi'_M T$ , the appearance of an out-of-phase signal ( $\chi''_M$ ) is observed. A frequency-dependent drop in the in-phase ( $\chi'_M T$ ) component and an appearance of an out-of-phase ( $\chi''_M$ ) component of the AC magnetic susceptibility are indicators of a SMM. The  $\chi''_M$  peak maximum is the temperature at which the frequency of the oscillating field equals the rate at which a single-molecule reverses its direction of magnetization. The maximum in the  $\chi''_M$  signal occurs at 3.1 K with a value of  $4.9 \text{ cm}^3 \text{ mol}^{-1}$  at 50 Hz. For the AC frequency range, 4–1500 Hz, the  $\chi''_M$  peaks of complex **5** occur in the range of 2–4.2 K. Almost all  $[\text{Mn}_{12}\text{O}_{12}(\text{O}_2\text{CR})_{16}(\text{H}_2\text{O})_4]$  complexes as well as **2** exhibit an out-of-phase peak in the 4–7 K range

[12,13]. This suggests that **5** has a relaxation rate greater than the latter complexes.

From the positions of the peak maximum in the  $\chi''_M$  versus  $T$  plot, values of the magnetization relaxation time  $\tau$  can be determined at various temperatures. Fig. 5 gives the resulting Arrhenius plot of  $\ln(1/\tau)$  versus  $1/T$  for complex **5**. The data were least-squares fit to the Arrhenius equation (Eq. (1)) to give  $\tau_0 = 5.9 \times 10^{-9}$  s and  $U_{\text{eff}} = 28 \text{ cm}^{-1} = 41 \text{ K}$ ,

$$\frac{1}{\tau} = \frac{1}{\tau_0} \exp\left(\frac{-U_{\text{eff}}}{kT}\right) \quad (1)$$

where  $U_{\text{eff}}$  is the effective energy barrier for the magnetization relaxation. The normal range of  $U_{\text{eff}}$  for  $[\text{Mn}_{12}\text{O}_{12}(\text{O}_2\text{CR})_{16}(\text{H}_2\text{O})_4]$  complexes and complex **2** is  $U_{\text{eff}} = 42\text{--}50 \text{ cm}^{-1} = 60\text{--}72 \text{ K}$ . Thus, the  $U_{\text{eff}}$  for **5** is significantly lower and consistent with molecules possessing abnormal JT axes, i.e. the ‘faster relaxing’  $\text{Mn}_{12}$  complexes.

### 3. Conclusions

The preparation and X-ray structure have been reported for  $[\text{Mn}_{12}\text{O}_{12}(\text{O}_2\text{CC}_6\text{H}_5)_7(\text{O}_2\text{PPh}_2)_9(\text{H}_2\text{O})_4] \cdot 3\text{CH}_2\text{Cl}_2$  (**5**). It shows that a ninth bulky diphenylphosphinate group can be accommodated about the  $[\text{Mn}_{12}\text{O}_{12}]^{16+}$  core. Complex **5** also exhibits the abnormal orientation of two  $\text{Mn}^{\text{III}}$  JT axes towards oxide ligands, and is thus an example of the rarer type of JT isomer. DC magnetic measurements indicate the ground

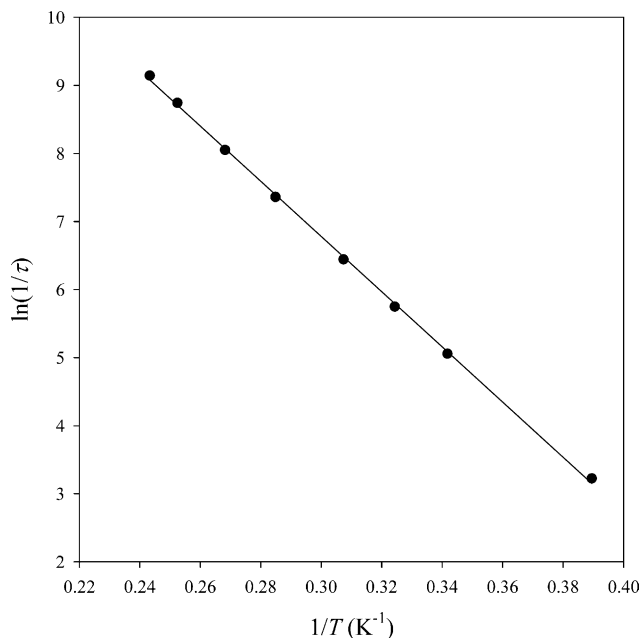


Fig. 5. Plot of the natural logarithm of relaxation rate,  $\ln(1/\tau)$  versus inverse temperature for complex **5** using the  $\chi''_M$  versus  $T$  data of Fig. 4. The solid line is a fit to the Arrhenius equation as described in the text.

state to be  $S = 10$  with  $D = -0.42 \text{ cm}^{-1} = -0.60 \text{ K}$ . AC magnetic measurements show a frequency-dependent out-of-phase signal, with peak maxima in only the 2–4.2 K range. The effective energy barrier ( $U_{\text{eff}} = 28 \text{ cm}^{-1} = 41 \text{ K}$ ) is smaller than normal  $\text{Mn}_{12}$  complexes, but similar to those for  $\text{Mn}_{12}$  complexes with abnormally oriented JT axes.

#### 4. Supplementary material

Crystallographic data for the structural analysis have been deposited with the Cambridge Crystallographic Data Centre, CCDC No. 194465. Copies of this information may be obtained from The Director, CCDC, 12 Union Road, Cambridge, CB2 1EZ, UK (fax: +44-1233-336033; e-mail: deposit@ccdc.com.ac.uk or www: <http://www.ccdc.cam.ac.uk>).

#### References

- [1] R. Sessoli, H.-L. Tsai, A.R. Schake, S. Wang, J.B. Vincent, K. Folting, D. Gatteschi, G. Christou, D.N. Hendrickson, *J. Am. Chem. Soc.* 115 (1993) 1804.
- [2] R. Sessoli, K. Gatteschi, A. Caneschi, M.A. Novak, *Nature* 365 (1993) 141.
- [3] S.M.J. Aubin, M.W. Wemple, D.M. Adams, H.-L. Tsai, G. Christou, D.N. Hendrickson, *J. Am. Chem. Soc.* 118 (1996) 7746.
- [4] J.R. Friedman, M.P. Sarachik, *Phys. Rev. Lett.* 76 (1996) 3830.
- [5] L. Thomas, F. Lioni, R. Ballou, D. Gatteschi, R. Sessoli, B. Babara, *Nature* 383 (1996) 145.
- [6] J. Tejada, R.F. Ziolo, X.X. Zhang, *Chem. Mater.* 8 (1996) 1784.
- [7] H.J. Eppley, H.-L. Tsai, N. de Vries, K. Folting, G. Christou, D.N. Hendrickson, *J. Am. Chem. Soc.* 117 (1995) 301.
- [8] M. Soler, S.K. Chandra, D. Ruiz, E.R. Davidson, D.N. Hendrickson, G. Christou, *Chem. Commun.* (1998) 803.
- [9] M. Soler, P. Artus, K. Folting, J.C. Huffman, D.N. Hendrickson, G. Christou, *Inorg. Chem.* 40 (2001) 4902.
- [10] P. Artus, C. Boskovic, J. Yoo, W.E. Streib, L.-C. Brunel, D.N. Hendrickson, G. Christou, *Inorg. Chem.* 40 (2001) 4199.
- [11] C. Boskovic, M. Pink, J.C. Huffman, D.N. Hendrickson, G. Christou, *J. Am. Chem. Soc.* 123 (2001) 9914.
- [12] N. Chakov, K.A. Abboud, D.N. Hendrickson, G. Christou, *Dalton Trans.*, in press.
- [13] Z. Sun, D. Ruiz, N.R. Dilley, M. Soler, J. Ribas, K. Folting, M.B. Maple, G. Christou, D.N. Hendrickson, *Chem. Commun.* (1999) 1973.
- [14] S.M.J. Aubin, Z. Sun, H.J. Eppley, E.M. Rumberger, I.A. Guzei, K. Folting, P.K. Gantzel, A.L. Rheingold, G. Christou, D.N. Hendrickson, *Inorg. Chem.* 40 (2001) 2127.
- [15] J.B. Vincent, C. Christmas, H.-R. Chang, Q. Li, P.D.W. Boyd, J.C. Huffman, D.N. Hendrickson, G. Christou, *J. Am. Chem. Soc.* 111 (1989) 2086.